

Ground and Excited State Electronic Interactions in a Bis(phenanthroline) Copper(I) Complex Sandwiched between Two Fullerene Subunits

Yannick Rio, Gérald Enderlin, Cyril Bourgogne, and Jean-François Nierengarten*

Groupe de Chimie des Fullerènes et des Systèmes Conjugués, Ecole Européenne de Chimie, Polymères et Matériaux (ECPM), Université Louis Pasteur et CNRS, UMR 7504 (IPCMS), 25 Rue Becquerel, 67087 Strasbourg Cedex 2, France

Jean-Paul Gisselbrecht and Maurice Gross

Laboratoire d'Electrochimie et de Chimie Physique du Corps Solide, Université Louis Pasteur et CNRS (UMR 7512), 4 Rue Blaise Pascal, 67070 Strasbourg Cedex, France

Gianluca Accorsi and Nicola Armaroli*

Istituto per la Sintesi Organica e la Fotoreattività, Laboratorio di Fotochimica, Consiglio Nazionale della Ricerche, via Gobetti 101, 40129 Bologna, Italy

Received October 2, 2003

A new fullerene-substituted phenanthroline ligand has been obtained by reaction of a phenanthroline derivative bearing a 1,3-phenylenebis(methylene)-tethered bis-malonate with C_{60} in a double Bingel cyclopropanation. The relative position of the two cyclopropane rings in the resulting bis-methanofullerene derivatives has been determined on the basis of the molecular symmetry (C_3) deduced from the 1H and ^{13}C NMR spectra. The corresponding Cu(I) complex **F–Cu–F** has been prepared in good yields by treatment of the ligand with $Cu(CH_3CN)_4BF_4$. In the resulting multicomponent system, both C_{60} moieties are in a tangential orientation relative to their bridging phenyl ring, and the central bis(phenanthroline)Cu(I) core is sandwiched between the two carbon spheres. The electrochemical properties of **F–Cu–F** suggest the existence of ground-state electronic interactions in this multicomponent array based on the mutual effects exerted by the fullerene units to the bis(2,9-diphenyl-1,10-phenanthroline)Cu(I) complex and vice versa. Close vicinity and electronic interactions between the inorganic core and the peripheral fullerene units are also suggested by increased electronic absorption around 430 nm. The distance between the two moieties is estimated to be 4.3 Å by molecular modeling studies. The excited-state properties of **F–Cu–F** have also been investigated. Photoinduced electron transfer from the central chromophore to the external fullerene units occurs but, surprisingly, only following population of the excited states of the central inorganic unit and not of the external carbon spheres. This is mainly attributed to kinetic factors related to the different nature of the two types of excited states involved, namely charge transfer (excitation on the metal-complexed moiety) vs a localized state (excitation on the fullerene units).

Introduction

In the last two decades, many covalently linked multicomponent arrays containing metal complexes have been synthesized. They have proven to be of great importance to

gain insight into the dynamics and mechanism of intramolecular photoinduced energy and electron transfer processes.^{1,2} In particular, several hybrid systems involving inorganic and organic molecular subunits have been prepared

* Corresponding authors. E-mail: jfnierengarten@chimie.u-strasbg.fr (J.-F.N.). Phone: + 33 390 242645 (J.-F.N.). Fax: + 33 390 242706 (J.-F.N.). E-mail: armaroli@isof.cnr.it.

(1) Scandola, F.; Chiorboli, C.; Indelli, M. T.; Rampi, M. A. In *Electron Transfer in Chemistry*; Balzani, V., Ed.; Wiley-VCH: Weinheim, 2001; Vol. 3, p 337.

(2) Barigelletti, F.; Flamigni, L. *Chem. Soc. Rev.* **2000**, 29, 1.

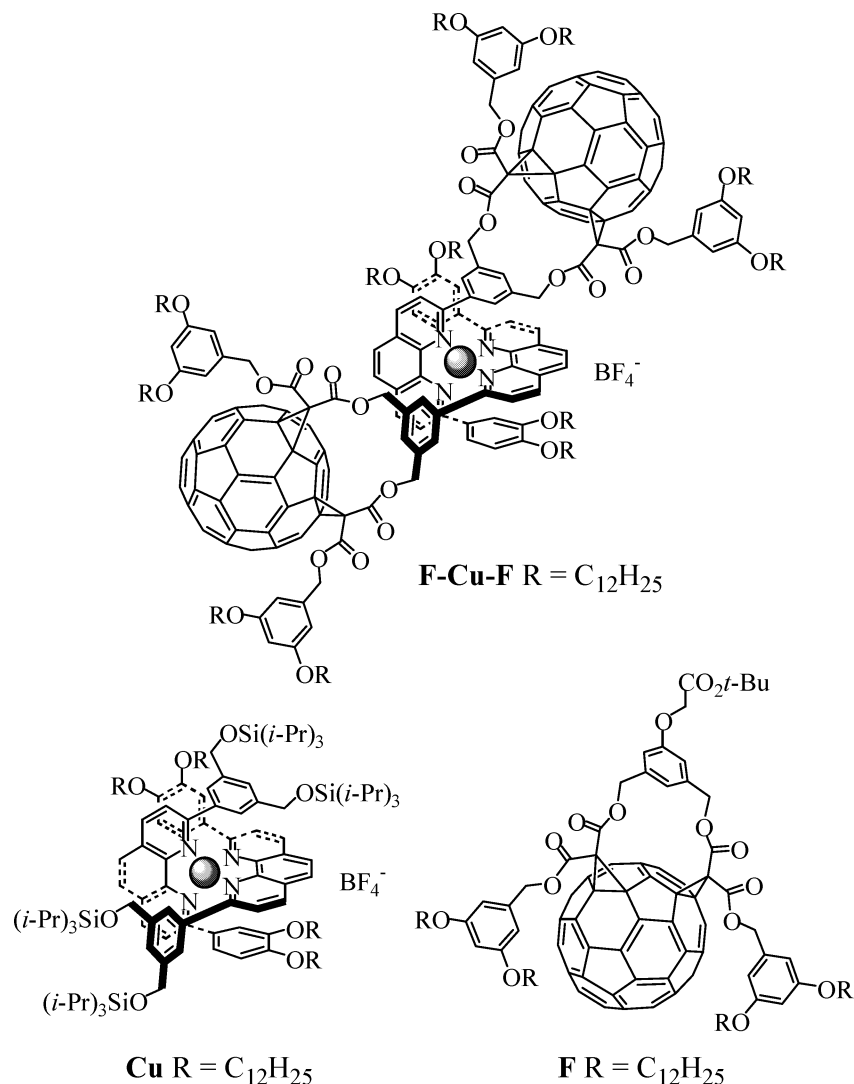


Figure 1. Compound **F-Cu-F** and the corresponding model compounds **Cu** and **F**.

in which the inorganic moiety is a coordination compound of d^6 metal ions [Ru(II), Os(II), Re(I)] that can act as light absorbing unit (chromophore), capable of starting up photo-induced processes.³ Depending on the electronic properties of the organic counterpart(s), two classes of such arrays have been singled out, which are conventionally called “chromophore-quencher” and “chromophore-sensitizer”.^{1,3} In the former case, the organic quencher is typically an electron donor or acceptor with no chromophoric character; in the latter case, the organic sensitizer is a chromophore itself and may transfer its excitation energy to the inorganic chromophoric counterpart.^{1,3}

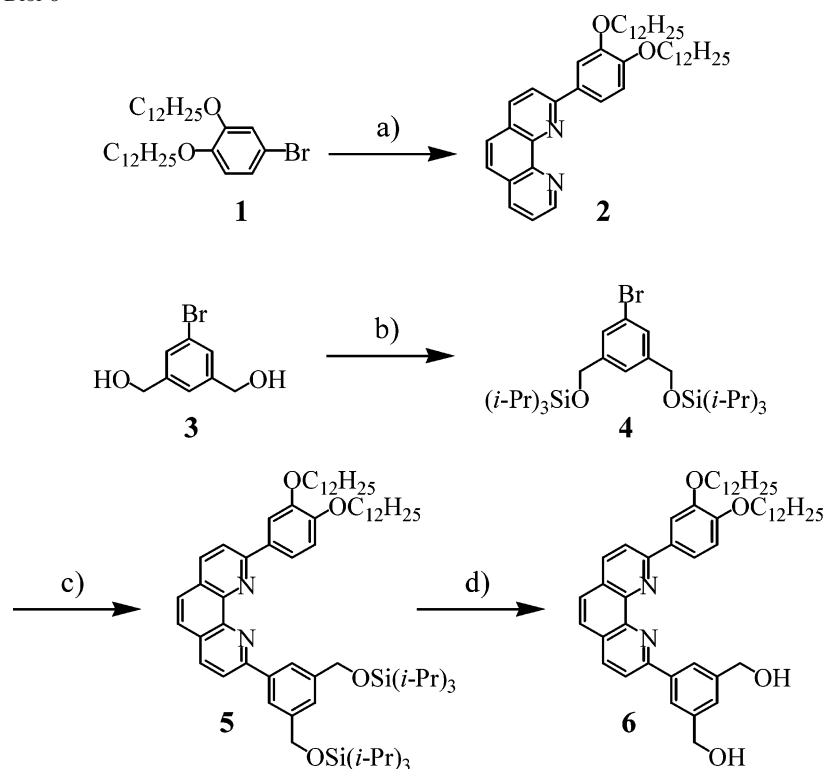
Recent developments in the synthesis of functionalized fullerenes have allowed the preparation of new families of organic–inorganic (hybrid) arrays, where the organic subunits are C_{60} fullerenes, while the inorganic chromophores can be Ru(II),^{4–6} Cu(I),^{7,8} or Re(I)⁶ complexes.⁹ Fullerenes

absorb light throughout the UV–vis spectral region, possess low-lying $\pi\pi^*$ singlet and triplet states, and are excellent electron acceptors. Such concomitant features are rather unique for organic molecules; thus, when one uses the above-mentioned classification for organic–inorganic hybrids containing fullerenes, one has to keep in mind that the roles of chromophore and quenchers/sensitizer can be exchanged between the organic and the inorganic units. Addressing light excitation to a given molecular component, i.e., choosing the chromophore, enables the assignment of the specific role of each partner.

Herein we describe the synthesis, the electrochemical, and the photophysical properties of a new organic–inorganic array **F-Cu-F** made of a Cu(I)–bisphenanthroline complex

- (3) *Photoinduced Electron Transfer in Metal-Organic Dyads*; Schanze, K. S., Walters, K. A., Eds.; Marcel Dekker: New York, 1998.
- (4) Maggini, M.; Guldi, D. M.; Mondini, S.; Scorrano, G.; Paolucci, F.; Ceroni, P.; Roffia, S. *Chem. Eur. J.* **1998**, *4*, 1992.
- (5) Guldi, D. M.; Maggini, M.; Menna, E.; Scorrano, G.; Ceroni, P.; Marcaccio, M.; Paolucci, F.; Roffia, S. *Chem. Eur. J.* **2001**, *7*, 1597.

- (6) Armaroli, N.; Accorsi, G.; Felder, D.; Nierengarten, J. F. *Chem. Eur. J.* **2002**, *8*, 2314.
- (7) Armaroli, N.; Diederich, F.; Dietrich-Buchecker, C. O.; Flamigni, L.; Marconi, G.; Nierengarten, J. F.; Sauvage, J. P. *Chem. Eur. J.* **1998**, *4*, 406.
- (8) Armaroli, N.; Boudon, C.; Felder, D.; Gisselbrecht, J. P.; Gross, M.; Marconi, G.; Nicoud, J. F.; Nierengarten, J. F.; Vicinelli, V. *Angew. Chem., Int. Ed.* **1999**, *38*, 3730.
- (9) Meijer, M. D.; van Klink, G. P. M.; van Koten, G. *Coord. Chem. Rev.* **2002**, *230*, 141.

Scheme 1. Preparation of Diol 6^a

^a Reagents and conditions: (a) *t*-BuLi, THF, -78 to 0 °C, 3 h, then 1,10-phenanthroline, 0 °C, 3 h, then H_2O , then MnO_2 (78%); (b) TIPSCl, imidazole, DMF, 0 °C, 48 h (93%); (c) *t*-BuLi, THF, -78 to 0 °C, 3 h, then **2**, 0 °C, 5 h, then H_2O , then MnO_2 (75%); (d) TBAF, THF, 0 °C, 30 min (quantitative).

(Cu) sandwiched between two fullerene subunits (F) (Figure 1). Interestingly, owing to the unique structural features of F–Cu–F, ground-state electronic interactions between the two types of subunits are observed. The excited-state properties of F–Cu–F have also been investigated and compared to those of the corresponding model compounds F and Cu (Figure 1). When the Cu-complexed core is excited, F–Cu–F exhibits photoinduced electron transfer from the inorganic to the organic moieties. In contrast, excitation of the carbon spheres does not bring about any photoinduced processes. Thus, although both the inorganic and the organic units can start up electron transfer, only the former moiety turns out to be an effective chromophore in triggering the excited state interaction.

Results and Discussion

Synthesis. In order to control the distance and the orientation of the different components in F–Cu–F, it was decided to connect one of the phenyl groups of both phenanthroline ligands to two points of the surface of their fullerene substituent. In this way, both C_{60} moieties are in a tangential orientation relative to their bridging phenyl ring and the central bis(phenanthroline)Cu(I) core is thus sandwiched between the two carbon spheres. The phenanthroline ligand precursor of F–Cu–F was obtained by taking advantage of the versatile regioselective reaction developed in the group of Diederich^{10,11} which led to C_{60} bis-adducts by a cyclization reaction at the C sphere with bis-malonates

in a double Bingel¹² cyclopropanation. To this end, a phenanthroline derivative substituted with a 1,3-phenylenebis-(methylene)-tethered bis-malonate was prepared by an esterification reaction between diol **6** and a malonic acid mono-ester derivative. The synthesis of the key intermediate **6** is depicted in Scheme 1. Treatment of 1-bromo-3,4-didodecyloxybenzene (**1**) with *t*-BuLi followed by reaction of the resulting 1-lithio-3,4-didodecyloxybenzene with 1,10-phenanthroline under the conditions developed by Sauvage and co-workers¹³ gave **2** in 78% yield. Treatment of diol **3**¹⁴ with triisopropylsilyl chloride (TIPSCl) in the presence of imidazole afforded the protected derivative **4** in 93% yield. Halogen–lithium exchange was achieved by reaction of **4** with *t*-BuLi. Subsequent addition of the resulting organolithium derivative to **2** followed by hydrolysis and rearomatization with MnO_2 gave **5** in 75% yield. Diol **6** was then obtained in a quantitative yield by treatment with tetra-*n*-butylammonium fluoride (TBAF) in THF at 0 °C.

Reaction of diol **6** with malonic acid mono-ester **7**¹⁵ under esterification conditions using *N,N'*-dicyclohexylcarbodiimide (DCC) and 4-(dimethylamino)pyridine (DMAP) in CH_2Cl_2 gave bis-malonate **8** in 73% yield. Finally, reaction of **8** with

(10) Nierengarten, J. F.; Gramlich, V.; Cardullo, F.; Diederich, F. *Angew. Chem., Int. Ed. Engl.* **1996**, *35*, 2101.

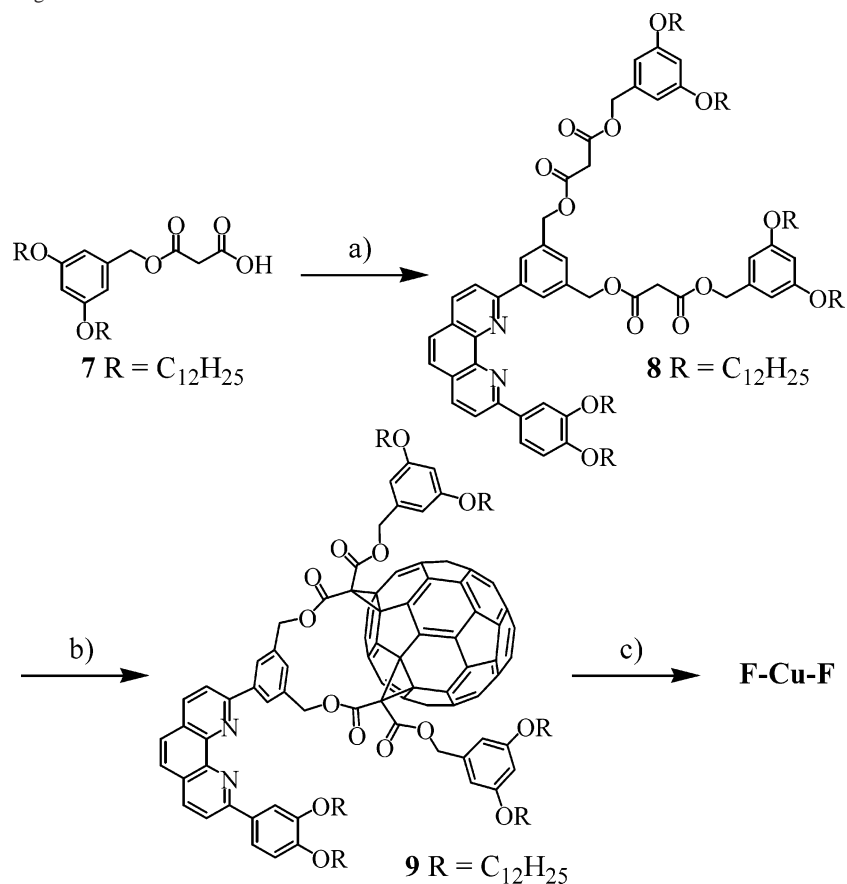
(11) Nierengarten, J. F.; Habicher, T.; Kessinger, R.; Cardullo, F.; Diederich, F.; Gramlich, V.; Gisselbrecht, J. P.; Boudon, C.; Gross, M. *Helv. Chim. Acta* **1997**, *80*, 2238.

(12) Bingel, C. *Chem. Ber.* **1993**, *126*, 1957.

(13) Marnot, P. A.; Dietrich-Buchecker, C. O.; Sauvage, J. P. *Tetrahedron Lett.* **1982**, *23*, 5291.

(14) Sherrod, S. A.; da Costa, R. L.; Barnes, R. A.; Boekelheide, V. J. *Am. Chem. Soc.* **1974**, *96*, 1565.

(15) Felder, D.; Nava, M. G.; Carreon, M. D.; Eckert, J. F.; Luccisano, M.; Schall, C.; Masson, P.; Gallani, J. L.; Heinrich, B.; Guillon, D.; Nierengarten, J. F. *Helv. Chim. Acta* **2002**, *85*, 288.

Scheme 2. Preparation of Ligand **9**^a

^a Reagents and conditions: (a) **6**, DCC, DMAP, CH₂Cl₂, 0 °C to room temperature, 72 h (73%); (b) C₆₀, I₂, DBU, toluene, rt, 12 h (38%); (c) Cu(CH₃CN)₄BF₄, CH₃CN, CH₂Cl₂, rt, 1 h (92%).

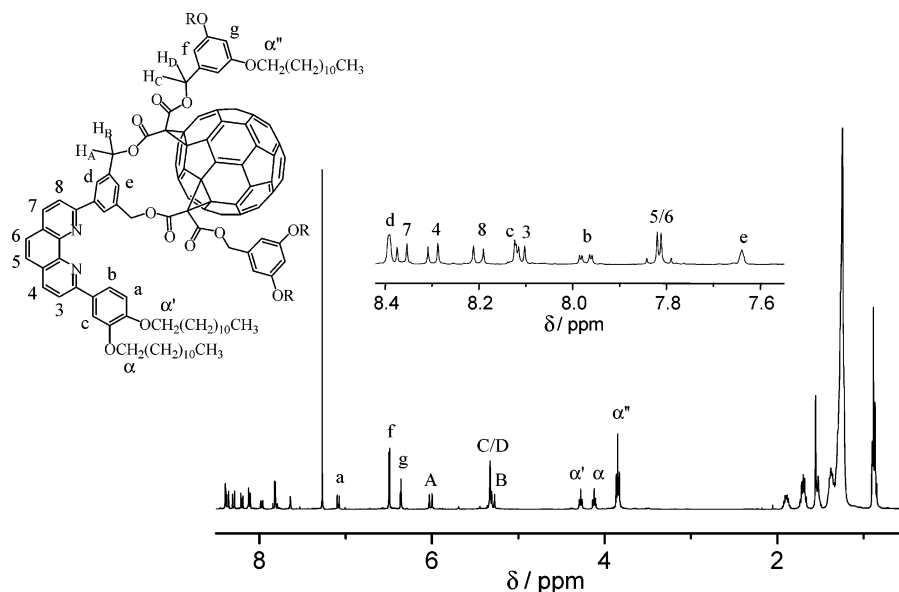


Figure 2. ¹H NMR spectrum (CDCl₃, 400 MHz) of the fullerene-functionalized phenanthroline derivative **9**.

C₆₀, I₂, and 1,8-diazabicyclo[5.4.0]undec-7-ene (DBU) in toluene at room temperature afforded the desired cyclization product **9** in 38% yield (Scheme 2).

Compound **9** was characterized by ¹H and ¹³C NMR, UV–vis, and IR spectroscopies. In addition, the structure of **9** was confirmed by FAB mass spectrometry. The relative position of the two cyclopropane rings in **9** on the C₆₀ surface

was determined on the basis of the molecular symmetry (C_s) deduced from the ¹H and ¹³C NMR spectra. The ¹H NMR spectrum of **9** is depicted in Figure 2. Unambiguous assignment was achieved on the basis of 2D-COSY and NOESY spectra recorded at room temperature in CDCl₃. The spectrum of **9** shows all the characteristic features of C_s symmetrical 1,3-phenylenebis(methylene)-tethered fullerene

cis-2 bis-adduct derivatives.^{15–18} Effectively, two sets of AB quartets are observed for the diastereotopic benzylic CH₂ groups (H_{A–B} and H_{C–D}) and an A₂X system is revealed for the aromatic protons of the 1,3,5-trisubstituted bridging phenyl ring (H_d and H_e). The spectrum is also characterized by three sets of AB quartets in the aromatic region in a typical pattern for a disymmetrical 2,9-disubstituted-1,10-phenanthroline (H_{3–4}, H_{5–6}, and H_{7–8}), an AMX system for the aromatic protons of the 3,4-didodecyloxyphenyl unit (H_a, H_b, and H_c), and an A₂X system for the aromatic protons of the 3,5-didodecyloxyphenyl rings (H_f and H_g).

The color and, accordingly, the absorption spectrum of a C₆₀ bis-adduct are highly dependent on the addition pattern and characteristic for each of the regioisomers.^{10,11,15} The orange color and the UV–vis spectrum of **9** are indeed fully consistent with those of previously reported analogous *cis*-2 bis-adducts.^{10,11,15–18}

The Cu(I) model complex **Cu** (Figure 1) was obtained in 96% yield by treatment of ligand **5** with Cu(CH₃CN)₄BF₄ in CH₂Cl₂/CH₃CN at room temperature. The coordination of **5** to the Cu(I) cation was easily observed by apparition of the metal-to-ligand charge transfer (MLCT) band characteristic of bis(2,9-diphenyl-1,10-phenanthroline)Cu(I) derivatives (see below). Furthermore, the ¹H NMR spectrum of **Cu** provided also good evidence for its formation. Effectively, as a result of the ring current effect of one phenanthroline subunit on the 2,9-substituents of the second one in the complex, the signals of the protons belonging to the phenyl rings attached to the phenanthroline core are shielded about 1.0–1.5 ppm in **Cu** when compared to the corresponding signals in ligand **5**. This particular behavior is specific to such copper(I) complexes.¹⁹

Compound **F–Cu–F** was also obtained by treatment of the corresponding ligand (**9**) with Cu(CH₃CN)₄BF₄. The ¹H NMR spectrum of complex **F–Cu–F** is consistent with the proposed structure. As observed for **Cu**, the resonances of the protons belonging to the phenyl rings attached to the phenanthroline unit are shielded about 1.0–1.5 ppm in the ¹H NMR spectrum of **F–Cu–F** when compared to the corresponding signals in the spectrum of **9**. In addition, it can be noted that compound **F–Cu–F** is C₂ symmetric and therefore chiral. As a result, the two equivalent fullerene *cis*-2 bis-adduct moieties have lost their plane of symmetry. For this reason, some of the protons that were equivalent in ligand **9** are not equivalent any longer in the complex and give rise to two sets of signals (H_d, H_A, H_B, H_C, H_D, H_f, and H_g, see Figure 2 for the assignment). The structure of **F–Cu–F** was also confirmed by mass spectrometry. As shown in Figure 3, the MALDI-TOF mass spectrum of **F–Cu–F** displays a singly charged ion peak at *m/z* 5198.6 which can be assigned

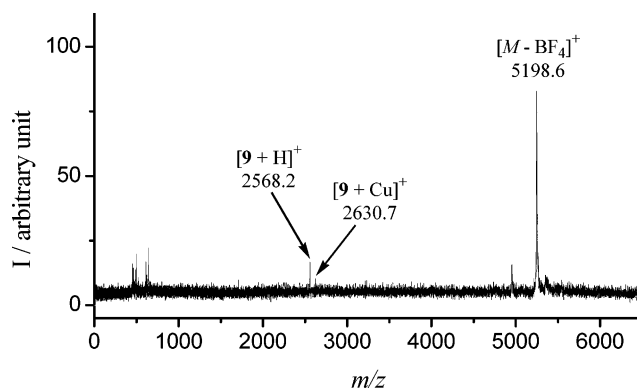


Figure 3. MALDI-TOF mass spectrum of **F–Cu–F**.

Table 1. Electrochemical Properties Determined by CV on a Glassy Carbon Working Electrode in CH₂Cl₂ + 0.1 M *n*Bu₄NPF₆ Solutions at Room Temperature

compd	reduction			oxidation
	<i>E</i> ₃	<i>E</i> ₂	<i>E</i> ₁	<i>E</i> ₁
Cu			–2.15 ^a	+0.37 ^a
9	–1.95 ^b	–1.51 ^b	–1.13 ^a	
F–Cu–F	–1.91 ^{b,c}	–1.41 ^{b,c}	–1.06 ^{a,c}	+0.44 ^a

^a Values for (*E*_{pa} + *E*_{pc})/2 in V vs Fc/Fc⁺ at a scan rate of 0.1 V s^{–1}.
^b Irreversible process, *E*_{pc} value reported. ^c Dielectronic process.

to the Cu(I) complex **F–Cu–F** after loss of the tetrafluoroborate counteranion ([M – BF₄]⁺, calculated for C₃₅₆H₃₅₂O₂₈N₄Cu: 5198.3). Two characteristic fragments are also observed. The first one at *m/z* 2568.2 corresponds to the free protonated ligand ([**9** + H]⁺) and the second one at *m/z* 2630.7 to the ligand coordinating a Cu(I) cation ([**9** + Cu]⁺). It can be noted that this fragmentation pattern is typically observed for such Cu(I) complexes.²⁰ However, when compared to mass spectra recorded under much harsher FAB conditions, the intensity of these two fragmentation peaks is very small in the MALDI-TOF mass spectrum, thus showing that the latter technique is an ideal tool for the characterization of such high molecular weight compounds.

Electrochemistry. The electrochemical properties of **Cu**, **9**, and **F–Cu–F** were investigated by cyclic voltammetry (CV) in CH₂Cl₂ + 0.1 M *n*Bu₄NPF₆ solutions. The results are summarized in Table 1.

In the anodic region, the copper(I) complex **F–Cu–F** shows a reversible one-electron process at +0.44 V vs Fc/Fc⁺ assigned to the oxidation of the metal center.^{8,21–23} Interestingly, the Cu-based oxidation appears to be significantly more anodic ($\Delta E = 70$ mV) with respect to the corresponding model compound **Cu**. The oxidation of Cu(I) to Cu(II) is accompanied by rearrangement from nearly tetrahedral to distorted square planar geometry.²⁴ However,

(16) Nierengarten, J. F.; Schall, C.; Nicoud, J. F. *Angew. Chem., Int. Ed.* **1998**, *37*, 1934.

(17) Nierengarten, J. F.; Eckert, J. F.; Felder, D.; Nicoud, J. F.; Armaroli, N.; Marconi, G.; Vicinelli, V.; Boudon, C.; Gisselbrecht, J. P.; Gross, M.; Hadziioannou, G.; Krasnikov, V.; Ouali, L.; Echegoyen, L.; Liu, S. G. *Carbon* **2000**, *38*, 1587.

(18) Nierengarten, J. F.; Oswald, L.; Nicoud, J. F. *Chem. Commun.* **1998**, 1545.

(19) Dietrich-Buchecker, C. O.; Marnot, P. A.; Sauvage, J.-P.; Kintzinger, J.-P. *Nouv. J. Chem.* **1984**, *8*, 573.

(20) Moucheron, C.; Dietrich-Buchecker, C. O.; Sauvage, J. P.; Van Dorsselaer, A. *J. Chem. Soc., Dalton Trans.* **1994**, 885.

(21) Dietrich-Buchecker, C. O.; Sauvage, J. P.; Kern, J. M. *J. Am. Chem. Soc.* **1989**, *111*, 7791.

(22) Federlin, P.; Kern, J. M.; Rastegar, A.; Dietrich-Buchecker, C.; Marnot, P. A.; Sauvage, J. P. *New J. Chem.* **1990**, *14*, 9.

(23) Dietrich-Buchecker, C. O.; Nierengarten, J. F.; Sauvage, J. P.; Armaroli, N.; Balzani, V.; De Cola, L. *J. Am. Chem. Soc.* **1993**, *115*, 11237.

(24) Armaroli, N. *Chem. Soc. Rev.* **2001**, *30*, 113.

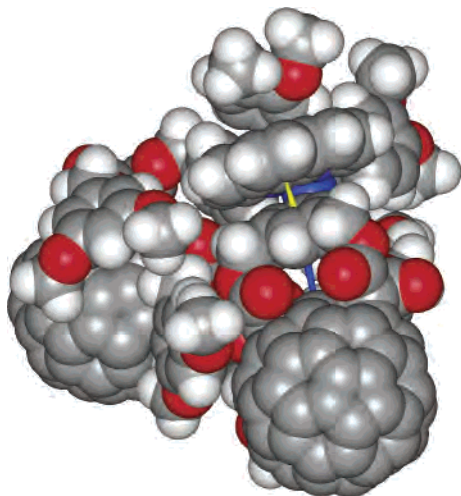


Figure 4. Snapshot of the theoretical structure of **F-Cu-F** at 300 K obtained from a Molecular Dynamics calculation showing the fullerene-phenyl-phenanthroline-phenyl stacking (the dodecyloxy groups have been replaced by methoxy substituents for clarity). The shortest distance between the fullerene sphere and its bridging phenyl ring (blue line) is 4.3 Å; the distance from the center of the phenyl ring of one ligand to the center of the central six-membered ring of the phenanthroline of the other ligand (yellow line) is 3.9 Å.

this process is not expected to be strongly affected by bulky substituents, when they are not directly attached to the phenanthroline ligand.²⁵ The observed potential shift is thus attributed to the strong electron-withdrawing effect of the fullerene units which destabilizes the Cu(II) state of the complex, as previously seen for C₆₀-porphyrin conjugates bearing similar *cis*-2 fullerene bis-adducts.^{17,18} This hypothesis is corroborated by the photophysical measurements which revealed the existence of sizable intramolecular electronic interactions in **F-Cu-F** (vide infra). Notably, molecular modeling studies show that the fullerene units are in tight vicinity to the bis(2,9-diphenyl-1,10-phenanthroline)Cu(I) complex (Figure 4). Effectively, the distance of the fullerene sphere to the center of its bridging phenyl ring is estimated to be 4.3 Å showing that they are close to being at the van der Waals contact. Therefore, it appears reasonable to ascribe the observed shift for the metal centered oxidation in **F-Cu-F** to electronic interactions between the bis(2,9-diphenyl-1,10-phenanthroline)Cu(I) core and the fullerene units.

As far as the reduction potential is concerned, **F-Cu-F** and model compound **9** show a similar behavior totally consistent with previously reported data for fullerene *cis*-2 bis-adducts.^{17,18,26} It can be noted that the two fullerene subunits in **F-Cu-F** behave as independent redox centers. Surprisingly, the reduction potentials are shifted to more positive values for **F-Cu-F** ($\Delta E = 70$ mV for the first reduction) when compared to fullerene derivative **9**. The latter observation seems to be in contradiction with the electronic interactions between the bis(2,9-diphenyl-1,10-phenanthroline)Cu(I) core and the fullerene units deduced

(25) Armaroli, N.; Accorsi, G.; Gisselbrecht, J. P.; Gross, M.; Eckert, J. F.; Nierengarten, J. F. *New J. Chem.* **2003**, *27*, 1470.

(26) Cardullo, F.; Seiler, P.; Isaacs, L.; Nierengarten, J. F.; Haldimann, R. F.; Diederich, F.; MordasiniDenti, T.; Thiel, W.; Boudon, C.; Gisselbrecht, J. P.; Gross, M. *Helv. Chim. Acta* **1997**, *80*, 343.

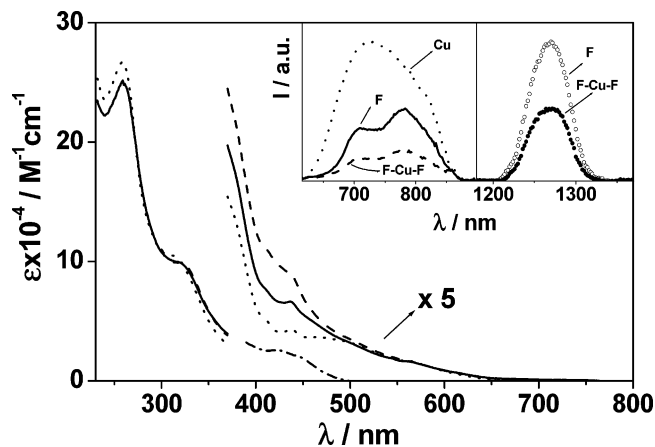


Figure 5. Absorption spectrum of **F-Cu-F** in CH₂Cl₂ (—) and benzonitrile (---), compared to the sum spectrum of **2F + Cu** (····) in CH₂Cl₂; the profile obtained by subtracting the sum spectrum to the experimental one is (— · — · —). Inset: emission spectra in CH₂Cl₂; fullerene fluorescence and MLCT band (left), sensitized singlet oxygen luminescence (right), $\lambda_{exc} = 600$ nm, $A = 0.190$ for all samples, light partitioning in **F-Cu-F** is 0.5:1:0.5. The emission properties of **F** are the same as for **9**.

from the oxidation potential of the metal center. Effectively, the reduction potentials are expected at a more negative value in such a case. However, one has to consider the proximity of the positively charged Cu(I) cation. Actually, Diederich and Echegoyen have reported positive shifts in the fullerene reduction potential ($\Delta E = 90$ mV) of a C₆₀-dibenzo-18-crown-6 conjugate upon complexation of a potassium cation due to the electrostatic effect of K⁺ bound in close proximity to the carbon sphere.^{27,28} Similarly, the positive shift in potential observed for the reduction of **F-Cu-F** relative to the uncomplexed compound **9** is attributed to an electrostatic effect able to counterbalance the electronic interactions between the bis(2,9-diphenyl-1,10-phenanthroline)Cu(I) core and the C₆₀ units that tend to negatively shift the reduction potentials.

Photophysical Properties. The electronic absorption spectrum of **F-Cu-F** in CH₂Cl₂ is reported in Figure 5.

Good matching with the profile obtained by summing the spectra of the model compounds **Cu** and **F** (1:2 ratio) is observed everywhere but in the region around 430 nm. Upon subtraction, the band depicted in Figure 5 is obtained. This can be attributed to electronic donor-acceptor interactions, as observed for some fullerene host-guest complexes²⁹ and in fullerodendrimers where the external branches wrap the central carbon sphere.³⁰⁻³² The increased band intensity in polar benzonitrile (Figure 5) corroborates this assignment.³³ Notably, donor-acceptor multicomponent arrays containing

(27) Bourgeois, J. P.; Seiler, P.; Fibbioli, M.; Pretsch, E.; Diederich, F.; Echegoyen, L. *Helv. Chim. Acta* **1999**, *82*, 1572.

(28) Bourgeois, J. P.; Echegoyen, L.; Fibbioli, M.; Pretsch, E.; Diederich, F. *Angew. Chem., Int. Ed.* **1998**, *37*, 2118.

(29) Eckert, J. F.; Byrne, D.; Nicoud, J. F.; Oswald, L.; Nierengarten, J. F.; Numata, M.; Ikeda, A.; Shinkai, S.; Armaroli, N. *New J. Chem.* **2000**, *24*, 749.

(30) Rio, Y.; Accorsi, G.; Nierengarten, E.; Rehspringer, J.-L.; Hönerlage, B.; Kopitkovas, G.; Chugreev, A.; Van Dorsselaer, A.; Armaroli, N.; Nierengarten, J. F. *New J. Chem.* **2002**, *26*, 1146.

(31) Murata, Y.; Ito, M.; Komatsu, K. *J. Mater. Chem.* **2002**, *12*, 2009.

(32) Rio, Y.; Accorsi, G.; Nierengarten, H.; Bourgoigne, C.; Strub, J.-M.; Van Dorsselaer, A.; Armaroli, N.; Nierengarten, J.-F. *Tetrahedron* **2003**, *59*, 3833.

fullerenes rarely present high-energy^{30,31} or low-energy^{33–35} CT absorption bands, and this happens only when a contact distance between donor–acceptor partners is possible. Thus, our results are in good agreement with the molecular modeling studies showing that the fullerene units are in tight vicinity to the central Cu(I) complex in **F–Cu–F** (Figure 4).

Both kind of molecular subunits of **F–Cu–F** are luminescent. At 298 K, **Cu** exhibits an emission band ($\lambda_{\text{max}} = 726$ nm, $\tau = 199$ ns, and $\Phi_{\text{em}} = 8.5 \times 10^{-4}$ in air-free CH_2Cl_2 solution) originating from the deactivation of a thermally equilibrated manifold of the lowest singlet and triplet metal-to-ligand charge-transfer states (¹MLCT and ³MLCT), separated by about 1500 cm^{-1} .^{24,36,37} At 77 K, the emission band, red shifted and very weak ($\lambda_{\text{max}} = 760$ nm, $\tau = 1.6\ \mu\text{s}$), is attributed to the ³MLCT level.^{37,38} At 298 K, dimethanofullerene **F** exhibits a structured fluorescence band with the highest energy feature peaking at 706 nm ($\tau = 1.5$ ns, $\Phi_{\text{em}} = 3.0 \times 10^{-4}$, CH_2Cl_2), substantially unmodified at 77 K.⁸

The characteristic luminescence properties of the two reference compounds can conveniently signal the occurrence of intercomponent excited-state interactions in the **F–Cu–F** assembly. In Figure 5 are displayed the emission spectra of **Cu**, **F**, and **F–Cu–F** at $\lambda_{\text{exc}} = 600$ nm (isoabsorbing samples, $A = 0.190$), where light partitioning among the **Cu** and **F** chromophores in **F–Cu–F** is 0.5:1:0.5. Quenching of the MLCT-type emission band of the Cu(I)-complexed moiety is evidenced. On the contrary, the amount of light directly exciting the fullerene moieties (50%) gives rise to a fluorescence band exhibiting the same parameters as **F** (see above). The yield of fullerene triplet formation of **F–Cu–F** relative to **F** has been indirectly measured via the singlet oxygen method described earlier.⁶ Taking into account the 1:1 light sharing among the two types of chromophores, the yield of fullerene triplet formation is the same for **F–Cu–F** and **F** (Figure 5, inset); also the triplet lifetime is identical, i.e., 18.0 μs and 650 ns in air-free and air-equilibrated CH_2Cl_2 , respectively. Taken together, the above results show that (i) excitation of the Cu(I)-complexed core results in quenching of the MLCT excited states not followed by sensitization of the fullerene electronic levels; (ii) excitation of the external carbon spheres brings about regular deactivation of the C_{60} excited states, unmodified relative to **F**. The quenched lifetime of the MLCT level of **F–Cu–F** is determined to be 600 ps by time correlated single photon counting spectrometry, thus $k_q = 1.7 \times 10^9\text{ s}^{-1}$. Since no sensitization of the lower lying fullerene triplet state (1.40

eV)⁸ is evidenced, the quenching of the Cu-complexed moiety must be attributed to quantitative photoinduced electron-transfer process occurring from the lowest MLCT manifold, located at about 1.63 eV, to a lower-lying charge separated $\text{Cu}^+ - \text{F}^-$ localized at 1.50 eV, as estimated from the one-electron redox potentials³⁹ (Table 1). Unfortunately, we are unable to detect the charge recombination step since our current transient absorption apparatus has no spectral sensitivity above 1000 nm, where the fullerene radical anion diagnostic peak is located. On the other hand, the oxidized metal center is not expected to give observable absorption features, also considering that at 355 and 532 nm (Nd:YAG laser harmonics) most of the light (>60%) is absorbed by the fullerene chromophores, which are unable to trigger electron transfer and exhibit very strong singlet and triplet transient absorption features.

An energy level diagram reporting all the relevant electronic and charge separated states, as determined by luminescence and electrochemical potentials,³⁹ is reported in Figure 6. A certain degree of Coulombic interaction within the charge separated system may be present due to the short intercomponent distance and the medium-level polarity of CH_2Cl_2 .⁴⁰ A quantitative estimation of this effect is subject to severe approximations,⁴¹ and we prefer to neglect such contribution, keeping in mind that some stabilization of the charge separated state may occur with respect to what is indicated in Figure 6. For the Cu-complexed moiety, both the singlet and triplet state are reported; they are in thermal equilibration at room temperature, the population of the triplet being predominant.³⁸

The electron-transfer rate constant, according to the classical model of Marcus and Sutin, can be expressed as follows:⁴²

$$k_{\text{el}} = \nu_{\text{N}} \kappa \exp\left(\frac{\Delta G^\ddagger}{RT}\right) \quad (1)$$

where ν_{N} is the nuclear frequency factor of the reaction, which can be expressed as a weighted mean of the frequencies of the various nuclear modes involved in the reaction coordinate, κ is the transmission coefficient of the reaction which describes the probability that the reactants, once they reach the geometry of the crossing point between potential energy surfaces, convert into products; ΔG^\ddagger is the activation energy of the electron-transfer process.

According to electrochemical data and absorption spectra and in light of the short interchromophoric distance (4.3 Å), the electronic interaction between the metal center and the fullerene units in **F–Cu–F** is relatively high. Therefore, electron transfer can be expected to occur in the so-called adiabatic regime in which the rate determining step is the nuclear motion that leads to the transition-state geometry and the electronic transmission coefficient of the

(33) Armaroli, N.; Marconi, G.; Echegoyen, L.; Bourgeois, J. P.; Diederich, F. *Chem. Eur. J.* **2000**, *6*, 1629.

(34) Simonsen, K. B.; Konovalov, V. V.; Konovalova, T. A.; Kawai, T.; Cava, M. P.; Kispert, L. D.; Metzger, R. M.; Becher, J. *J. Chem. Soc., Perkin Trans. 2* **1999**, 657.

(35) Imahori, H.; Tkachenko, N. V.; Vehmanen, V.; Tamaki, K.; Lemmetyinen, H.; Sakata, Y.; Fukuzumi, S. *J. Phys. Chem. A* **2001**, *105*, 1750.

(36) Everly, R. M.; McMillin, D. R. *J. Phys. Chem.* **1991**, *95*, 9071.

(37) Felder, D.; Nierengarten, J. F.; Barigelletti, F.; Ventura, B.; Armaroli, N. *J. Am. Chem. Soc.* **2001**, *123*, 6291.

(38) Kirchhoff, J. R.; Gamache, R. E.; Blaskie, M. W.; Del Paggio, A. A.; Lengel, R. K.; McMillin, D. R. *Inorg. Chem.* **1983**, *22*, 2380.

(39) Balzani, V.; Scandola, F. *Supramolecular Photochemistry*; Ellis Horwood: Chichester, U.K., 1991; p 44.

(40) Kavarnos, G. J.; Turro, N. J. *Chem. Rev.* **1986**, *86*, 401.

(41) Koeberg, M.; de Groot, M.; Verhoeven, J. W.; Lokan, N. R.; Shephard, M. J.; Paddon-Row, M. N. *J. Phys. Chem. A* **2001**, *105*, 3417.

(42) Marcus, R. A.; Sutin, N. *Biochim. Biophys. Acta* **1985**, *811*, 265.

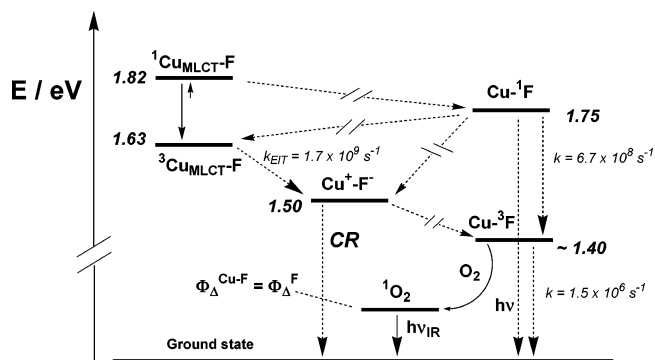


Figure 6. Energy level diagram for F-Cu-F and related photoinduced processes upon excitation of both chromophores. In the shorthand notations, only one F unit is indicated for F-Cu-F because under our experimental conditions, i.e., light intensity, only one F unit can be excited. The excited state energies of ${}^3\text{Cu}_{\text{MLCT}}\text{-F}$ and $\text{Cu-}^1\text{F}$ are estimated from the 77 K emission band maxima of Cu and F , respectively, that of ${}^1\text{Cu}_{\text{MLCT}}\text{-F}$ is located 1500 cm^{-1} above ${}^3\text{Cu}_{\text{MLCT}}\text{-F}$ (ref 38), and that of $\text{Cu-}^3\text{F}$ from theoretical calculations (ref 8). The position of the CS state is obtained from the electrochemical data.

reaction (K) is virtually unity.⁴⁰ ΔG^\ddagger is related to the thermodynamic driving force according to eq 2⁴²

$$\Delta G^\ddagger = \frac{\lambda}{4} \left(1 + \frac{\Delta G^\circ}{\lambda} \right)^2 \quad (2)$$

where λ is the reorganization energy, a term comprising two contributions, namely inner (bond length and angles) and outer (solvent orientation) nuclear rearrangements of the reacting pair.

From the energy diagram in Figure 6, it is evident that electron transfer occurring from $\text{Cu-}^1\text{F}$ and ${}^3\text{Cu}_{\text{MLCT}}\text{-F}$ are both moderately exergonic ($\Delta G^\circ = -0.25$ and -0.13 eV). In both cases, electron transfer can be safely located in the normal region of the Marcus parabola, even if some stabilization of the charge-separated state due to Coulombic interactions is present (see above); for example, compact hybrid fullerene-porphyrin arrays exhibit a λ value as large as 0.86 eV.⁴³ Thus a faster electron-transfer process from the fullerene singlet than from the MLCT state should occur, which is not the case. Indeed the longer lifetime of the MLCT manifold (199 ns) relative to the fullerene singlet (1.5 ns) should favor competitive deactivation pathways, such as electron transfer, versus internal deactivation. However the lifetime effect alone is not expected to play a crucial role, since the rate of electron-transfer deactivation of the MLCT state is 2.5 times faster than the rate of intrinsic decay of the fullerene singlet so, in principle, it is fast enough to expect substantial electron-transfer deactivation from the latter level, too.

We believe that the main reason for the observed asymmetric electron-transfer behavior may lie in the different nature of the two excited states, i.e., charge transfer vs localized. In particular, the preliminary formation of the MLCT state lowers the *external* reorganization energy demand, related to solvent repolarization around newly formed charged species. Even more importantly, one can expect a favorable impact on *internal* reorganization energy,

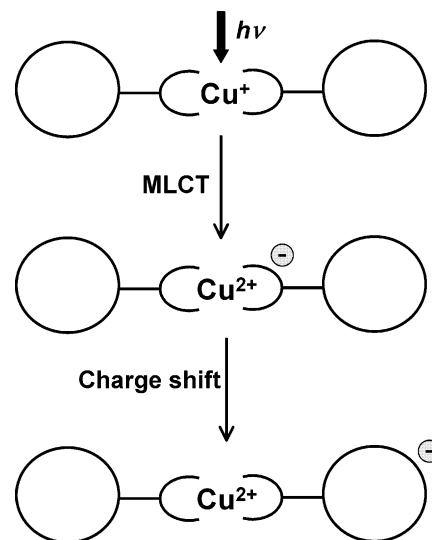


Figure 7. Schematic representation of the photoinduced processes observed in F-Cu-F .

related to molecular internal rearrangements following electron transfer. In fact, Cu(I) -phenanthroline complexes are known to undergo extensive structural rearrangements upon oxidation of Cu(I) to Cu(II) ,²⁴ due to the different coordination geometry of the two ions. All these effects on the total reorganization energy of a Marcus “normal region” electron-transfer process ($-\Delta G^\circ < \lambda$) contribute to lower the activation barrier ΔG^\ddagger toward the formation of $\text{Cu}^+\text{-F}^-$, when preliminary formation of a MLCT state is accomplished. On the contrary, when the carbon sphere is the chromophore and a localized ${}^1\pi\pi^*$ state is generated, electron transfer is comparably disfavored and fast internal deactivation prevails. Interestingly, enhancement of electron-transfer rate between two distant porphyrin units, separated by a $[\text{Cu}(\text{phen})_2]^+$ -type chromophore acting as primary electron acceptor, has been documented very recently.⁴⁴

Although in the adiabatic regime the intercomponent electronic coupling is not expected to play a significant role in determining the electron-transfer rate, it must be emphasized that the formation of the MLCT state prior to the final charge separation may contribute to yield a better electronic interaction between the two chromophores. In fact, the formation of the MLCT state implies redistribution of negative charge on the phenyl-phenanthroline ligand,⁴⁵ i.e., in the direction of the attached C_{60} electron acceptor. This makes the donor-acceptor distance effectively smaller, certainly not disfavoring the reaction kinetics. Similar electronic effects on the rate of photoinduced electron transfer have been recently observed for organic⁴⁶ and hybrid⁴⁷ donor-acceptor arrays. The electron-transfer process occurring in F-Cu-F upon excitation of the Cu(I) -complexed chromophore is schematized in Figure 7.

(44) Andersson, M.; Linke, M.; Chambron, J. C.; Davidsson, J.; Heitz, V.; Hammarström, L.; Sauvage, J. P. *J. Am. Chem. Soc.* **2002**, *124*, 4347.

(45) Gordon, C. K.; McGarvey, J. J. *Inorg. Chem.* **1991**, *30*, 2986.

(46) Lukas, A. S.; Zhao, Y. Y.; Miller, S. E.; Wasielewski, M. R. *J. Phys. Chem. B* **2002**, *106*, 1299.

(47) Flamigni, L.; Marconi, G.; Dixon, I. M.; Collin, J. P.; Sauvage, J. P. *J. Phys. Chem. B* **2002**, *106*, 6663.

(43) Guldi, D. M. *Chem. Soc. Rev.* **2002**, *31*, 22.

It must also be noted that the fullerene singlet state might be quenched by energy transfer to the $^3\text{MLCT}$ excited level (Figure 6), but this process is not observed. Such singlet–triplet energy transfer should occur via the double electron-exchange mechanism,⁴⁸ which is expected to be controlled by similar factors as electron transfer,⁴⁹ and thus disfavored as well. The present case interestingly compares to a Cu(I)–phenanthroline rotaxane bearing two fullerene stoppers, where quenching of the fullerene singlet state by energy transfer to the $^3\text{MLCT}$ level of the Cu(I)-complexed moiety was observed.⁷ The different behavior of the two systems may be attributed to substantial variations of interchromophoric distance, possibly affecting the ground- and excited-state distortion (and electronic properties) of the central metal chromophore.²⁴ Also, the electronic properties (e.g., absorption and emission spectra) of methanofullerenes and bismethanofullerenes are somewhat different.

As evidenced by the lack of singlet oxygen sensitization, the CS state of **F–Cu–F** is deactivated to the ground state and not to the fullerene triplet level, as found instead in fullerene dyads with Ru^{2+} or Re^+ coordination compounds.⁶ This suggests that fullerene/Cu(I)–phenanthroline dyads might be more promising candidates for the construction of photochemical devices for charge separation, since they are not suffering from the wasting sink effect of the fullerene triplet.⁶

Conclusion

A new fullerene-substituted phenanthroline ligand has been obtained by reaction of a phenanthroline derivative bearing a 1,3-phenylenebis(methylene)-tethered bis-malonate with C_{60} in a double Bingel cyclopropanation. The corresponding Cu(I) complex **F–Cu–F** has been prepared in good yields by treatment of the ligand with a Cu(I) salt. In this multicomponent system, both C_{60} moieties are in a tangential orientation relative to their bridging phenyl rings, and the central bis(phenanthroline)Cu(I) core is sandwiched between the two carbon spheres. Therefore, structural parameters such as the distance and the orientation of the different components in **F–Cu–F** are well defined. The electrochemical properties of **F–Cu–F** suggest the existence of ground-state donor–acceptor interactions in this multicomponent array based on the mutual effects exerted by the fullerene units to the bis(2,9-diphenyl-1,10-phenanthroline)Cu(I) complex and vice versa. The presence of a new absorption band in the UV–vis spectrum of **F–Cu–F** strengthens the hypothesis of strong electronic interactions between the inorganic core and the peripheral organic units, which is also supported by the short intercomponent distance derived by molecular modeling (4.3 Å). Electronic intramolecular interactions have been found in fullerene–metal cluster complexes⁵⁰ but are extremely rare in fullerene multicomponent arrays with nonplanar metal complexes.^{9,51} In **F–Cu–F**, photoinduced

electron transfer from the central metal-complexed chromophore to the external fullerene units may occur, in principle, by excitation of both moieties, but it is observed only following population of the excited states of the inorganic core. Photoexcitation of the peripheral carbon spheres is followed by “trivial” internal deactivation. The extensive internal and external (solvent) rearrangements that characterize the formation of MLCT excited states in Cu(I)-phenanthrolines are able to lead the reaction coordinates to favorable values so that electron transfer may proceed quickly. This effect is particularly favorable in **F–Cu–F** where the electronic interaction is not negligible and the gain of a suitable reaction geometry is crucial to promote electron transfer (adiabatic regime). These results show that hybrid organic–inorganic multicomponent arrays,⁵² due to profound differences in the nature of excited states, are particularly promising for the design of optoelectronic devices in which excitation of a given subunit triggers a specific and selective response.

Experimental Section

General Methods. Reagents and solvents were purchased as reagent grade and used without further purification. Compounds **F**,¹⁵ **1**,⁵³ **3**,¹⁴ and **7**¹⁵ were prepared according to previously reported procedures. All reactions were performed in standard glassware under an inert Ar atmosphere. Evaporation and concentration were done at water aspirator pressure and drying in vacuo at 10^{-2} Torr. Column chromatography: silica gel 60 (230–400 mesh, 0.040–0.063 mm) was purchased from E. Merck. Thin layer chromatography (TLC) was performed on glass sheets coated with silica gel 60 F_{254} purchased from E. Merck, visualization by UV light. IR spectra (cm^{-1}) were measured on an ATI Mattson Genesis Series FTIR instrument. NMR spectra were recorded on a Bruker AC 200 (200 MHz) or a Bruker AM 400 (400 MHz) with solvent peaks as reference. FAB-mass spectra (m/z ; % relative intensity) were taken on a ZA HF instrument with 4-nitrobenzyl alcohol as matrix. Mass measurement were carried out on a Bruker BIFLEX matrix-assisted laser desorption time-of-flight mass spectrometer (MALDI-TOF) equipped with SCOUT high-resolution optics, an X–Y multisample probe, and a gridless reflector. Ionization is accomplished with the 337 nm beam from a nitrogen laser with a repetition rate of 3 Hz. All data were acquired at a maximum accelerating potential of 20 kV in the linear positive ion mode. The output signal from the detector was digitized at a sampling rate of 1 GHz. A saturated solution of 1,8,9-trihydroxyanthracene (dithranol Aldrich EC: 214–538–0) in CH_2Cl_2 was used as a matrix. Typically, a 1/1 mixture of the sample solution in CH_2Cl_2 was mixed with the matrix solution, and 0.5 μL of the resulting mixture was deposited on the probe tip. Calibration was performed in the external mode with insulin (5734.6 Da) and ACTH (2465.2 Da). Elemental analyses were performed by the analytical service at the Institut Charles Sadron (Strasbourg, France).

Compound 2. A 1.7 M *t*-BuLi solution in pentane (7.9 mL, 13.4 mmol) was added by syringe to an argon-flushed, stirred solution of **1** (3.20 g, 6.1 mmol) in dry THF (60 mL) at -78°C . After 2 h, the resulting yellow solution was allowed to warm to 0°C (over 1

(48) Gilbert, A.; Baggott, J. *Essentials of Molecular Photochemistry*; Blackwell Scientific Publications: Oxford, U.K., 1991; p 176.

(49) Piotrowiak, P. In *Electron Transfer in Chemistry*; Balzani, V., Ed.; Wiley-VCH: Weinheim, 2001; Vol. 1, p 215.

(50) Lee, K.; Song, H.; Park, J. T. *Acc. Chem. Res.* **2003**, *36*, 78.

(51) Armaroli, N. *Photochem. Photobiol. Sci.* **2003**, *2*, 73.

(52) Liu, Y.; Li, Y.; Schanze, K. S. *J. Photochem. Photobiol., C* **2002**, *3*, 1.

(53) Yatabe, T.; Harbison, M. A.; Brand, J. D.; Wagner, M.; Mullen, K.; Samori, P.; Rabe, J. P. *J. Mater. Chem.* **2000**, *10*, 1519.

h), and then added under argon to a degassed solution of 1,10-phenanthroline (0.88 g, 4.9 mmol) in dry THF (20 mL) cooled to 0 °C (ice–water bath). The resulting dark red mixture was stirred for 3 h, and then hydrolyzed with water. CH₂Cl₂ was added, and the bright yellow organic layer decanted. The aqueous layer was extracted with CH₂Cl₂ (3×), and the combined organic layers were thereafter rearomatized by addition of MnO₂ (30 g), dried (MgSO₄), and filtered; the filtrate was then evaporated to dryness. Column chromatography on SiO₂ (CH₂Cl₂) yielded **2** (2.38 g, 78%) as a colorless glassy product. ¹H NMR (200 MHz, CDCl₃): 0.89 (t, *J* = 6 Hz, 6 H), 1.10–1.50 (m, 36 H), 1.86 (m, 4 H), 4.09 (t, *J* = 6 Hz, 2 H), 4.22 (t, *J* = 6 Hz, 2 H), 7.03 (d, *J* = 8 Hz, 1 H), 7.64 (dd, *J* = 8 and 4 Hz, 1 H), 7.79 (AB, *J* = 8 Hz, 2 H), 7.84 (dd, *J* = 8 and 2 Hz, 1 H), 7.91 (d, *J* = 2 Hz, 1 H), 8.06 (d, *J* = 8 Hz, 1 H), 8.25 (d, *J* = 8 Hz, 1 H), 8.29 (d, *J* = 8 Hz, 1 H), 9.23 (dd, *J* = 4 and 2 Hz, 1 H). ¹³C NMR (50 MHz, CDCl₃): 14.1, 22.7, 26.0, 26.1, 29.3, 29.4, 26.4, 29.7, 31.9, 69.2, 69.6, 113.5, 113.6, 120.3, 121.1, 122.8, 125.8, 126.4, 127.2, 129.0, 132.6, 136.0, 136.6, 146.0, 146.4, 149.4, 150.2, 150.7, 157.4. Anal. Calcd for C₄₂H₆₀O₂N₂·1/2H₂O: C 79.56, H 9.70, N 4.42. Found: C 79.66, H 9.61, N 4.29.

Compound 4. A mixture of TIPSCl (1.0 mL, 4.7 mmol), imidazole (0.59 g, 8.6 mmol), and **3** (0.47 g, 31.71 mmol) in DMF (15 mL) was stirred at room temperature for 48 h and evaporated. The residue was taken up with Et₂O, washed with brine, dried (MgSO₄), filtered, and evaporated. Column chromatography on SiO₂ (CH₂Cl₂/hexane 1:1) yielded **4** (1.06 g, 93%) as a colorless oil. ¹H NMR (200 MHz, CDCl₃): 0.90–1.20 (m, 42 H), 4.80 (s, 4 H), 7.40 (s, 3 H). ¹³C NMR (50 MHz, CDCl₃): 12.0, 18.0, 64.4, 121.6, 122.2, 127.2, 143.8. Anal. Calcd for C₂₆H₄₉Si₂O₂Br: C 59.06, H 9.35. Found: C 58.81, H 9.41.

Compound 5. A 1.7 M *t*-BuLi solution in pentane (2.3 mL, 3.9 mmol) was added by syringe to an argon-flushed, stirred solution of **4** (1.0 g, 1.9 mmol) in dry THF (15 mL) at –78 °C. After 2 h, the resulting yellow solution was allowed to warm to 0 °C (over 1 h), and then added under argon to a degassed solution of **2** (0.98 g, 1.5 mmol) in dry THF (15 mL) cooled to 0 °C (ice–water bath). The resulting dark red mixture was stirred for 5 h, and then hydrolyzed with water. CH₂Cl₂ was added and the bright yellow organic layer decanted. The aqueous layer was extracted with CH₂Cl₂ (3×), and the combined organic layers were thereafter rearomatized by addition of MnO₂ (30 g), dried (MgSO₄), and filtered; the filtrate was then evaporated to dryness. Column chromatography on SiO₂ (CH₂Cl₂/0.5% MeOH) yielded **5** (1.23 g, 75%) as a colorless glassy product. ¹H NMR (200 MHz, CDCl₃): 0.89 (t, *J* = 6 Hz, 6 H), 1.10–1.60 (m, 78 H), 1.89 (m, 4 H), 4.10 (t, *J* = 6 Hz, 2 H), 4.23 (t, *J* = 6 Hz, 2 H), 5.02 (s, 4 H), 7.04 (d, *J* = 7 Hz, 1 H), 7.68 (d, *J* = 2 Hz, 1 H), 7.78 (s, 2 H), 8.01 (d, *J* = 2 Hz, 1 H), 8.08 (dd, *J* = 7 and 2 Hz, 1 H), 8.13 (t, *J* = 2 Hz, 1 H), 8.14 (d, *J* = 7 Hz, 1 H), 8.23 (d, *J* = 2 Hz, 2 H), 8.27 (d, *J* = 7 Hz, 1 H), 8.31 (d, *J* = 7 Hz, 1 H). ¹³C NMR (50 MHz, CDCl₃): 12.1, 14.1, 18.1, 22.7, 26.1, 26.2, 29.3, 29.4, 29.5, 29.5, 29.7, 31.9, 65.3, 69.2, 69.5, 113.4, 119.6, 120.2, 121.0, 123.6, 124.5, 125.6, 125.9, 127.5, 127.9, 132.4, 136.7, 136.8, 139.1, 142.2, 145.9, 149.1, 150.8, 156.6, 157.1. Anal. Calcd for C₆₈H₁₀₈O₄N₂·H₂O: C 78.85, H 10.71, N 2.71. Found: C 78.76, H 10.81, N 2.69.

Compound 6. A 1 M TBAF solution in THF (3.7 mL, 3.7 mmol) was added to a stirred solution of **5** (1.18 g, 1.1 mmol) in THF (30 mL) at 0 °C. After 30 min, the reaction mixture was evaporated. The residue was taken up with CH₂Cl₂, washed with water, dried (MgSO₄), filtered, and evaporated. Column chromatography on SiO₂ (CH₂Cl₂/5% MeOH) yielded **6** (0.87 g, quantitative) as a colorless glassy product. ¹H NMR (200 MHz, CDCl₃): 0.88 (t, *J* = 7 Hz, 6

H), 1.10–1.60 (m, 36 H), 1.85 (m, 4 H), 2.21 (t, *J* = 6 Hz, 2 H), 4.09 (t, *J* = 6 Hz, 2 H), 4.25 (t, *J* = 6 Hz, 2 H), 4.81 (d, *J* = 6 Hz, 4 H), 7.04 (d, *J* = 8 Hz, 1 H), 7.46 (t, *J* = 2 Hz, 1 H), 7.76 (s, 2 H), 7.90 (dd, *J* = 8 and 2 Hz, 1 H), 8.06 (d, *J* = 8 Hz, 1 H), 8.11 (d, *J* = 2 Hz, 1 H), 8.13 (d, *J* = 8 Hz, 1 H), 8.25 (d, *J* = 8 Hz, 1 H), 8.29 (d, *J* = 8 Hz, 1 H), 8.35 (d, *J* = 2 Hz, 2 H). ¹³C NMR (50 MHz, CDCl₃): 14.1, 22.7, 26.1, 26.2, 29.4, 29.5, 29.7, 65.3, 69.2, 69.6, 113.3, 113.7, 119.9, 120.9, 125.3, 125.5, 126.2, 126.4, 127.5, 128.1, 132.4, 136.7, 139.9, 139.8, 141.8, 159.9, 149.4, 150.9, 156.1, 156.9. Anal. Calcd for C₅₀H₆₈O₄N₂: C 78.89, H 9.01, N 3.68, O 8.41. Found: C 78.70, H 9.13, N 3.64, O 8.71.

Compound 8. DCC (100 mg, 4.8 mmol) was added to a stirred solution of **6** (150 mg, 0.2 mmol), **7** (250 mg, 0.4 mmol), and DMAP (10 mg) in CH₂Cl₂ (35 mL) at 0 °C. After 1 h, the mixture was allowed to slowly warm to room temperature (within 1 h), then stirred for 72 h, filtered, and evaporated. Column chromatography on SiO₂ (hexane/CH₂Cl₂ 1:1) yielded **8** (270 mg, 73%) as a colorless glassy product. IR (CH₂Cl₂): 1727, 1746 (C=O). ¹H NMR (200 MHz, CDCl₃): 0.81 (m, 18 H), 1.10–1.60 (m, 108 H), 1.73 (m, 8 H), 1.88 (m, 4 H), 3.53 (s, 4 H), 3.88 (t, *J* = 6 Hz, 8 H), 4.11 (t, *J* = 6 Hz, 2 H), 4.20 (t, *J* = 6 Hz, 2 H), 5.10 (s, 4 H), 5.35 (s, 4 H), 6.37 (t, *J* = 2 Hz, 2 H), 6.44 (d, *J* = 2 Hz, 4 H), 7.09 (d, *J* = 8 Hz, 1 H), 7.48 (t, *J* = 2 Hz, 1 H), 7.80 (s, 2 H), 8.00–8.15 (m, 4 H), 8.28 (d, *J* = 7 Hz, 1 H), 8.31 (d, *J* = 7 Hz, 1 H), 8.42 (d, *J* = 2 Hz, 2 H). ¹³C NMR (50 MHz, CDCl₃): 14.1, 22.7, 26.0, 26.1, 26.2, 29.2, 29.3, 29.4, 29.5, 29.6, 29.6, 29.6, 29.7, 31.9, 41.5, 66.9, 67.2, 69.0, 69.1, 69.6, 101.1, 106.3, 106.6, 113.5, 113.6, 119.8, 119.9, 121.1, 125.5, 126.4, 127.4, 127.5, 128.17, 128.7, 132.3, 136.3, 136.7, 137.0, 137.2, 140.4, 145.9, 149.2, 151.0, 155.5, 156.9, 160.4, 166.2. Anal. Calcd for C₁₁₈H₁₈₀N₂O₁₄: C 76.58, H 9.80, N 1.51. Found: C 76.78, H 9.90, N 1.49.

Compound 9. DBU (0.1 mL, 0.6 mmol) was added to a stirred solution of C₆₀ (98 mg, 0.1 mmol), I₂ (80 mg, 0.3 mmol), and **8** (250 mg, 0.1 mmol) in toluene (200 mL) at room temperature. The solution was stirred for 12 h at room temperature, filtered through a short plug of SiO₂ (toluene then CH₂Cl₂/MeOH 95:5), and evaporated. Column chromatography on SiO₂ (CH₂Cl₂) yielded **12** (130 mg, 38%) as a dark orange glassy product. IR (CH₂Cl₂): 1740 (C=O). ¹H NMR (400 MHz, CDCl₃): 0.85 (m, 18 H), 1.15–1.65 (m, 108 H), 1.75 (m, 8 H), 1.88 (m, 4 H), 3.84 (t, *J* = 6 Hz, 8 H), 4.12 (t, *J* = 6 Hz, 2 H), 4.27 (t, *J* = 6 Hz, 2 H), 5.28 (d, *J* = 12 Hz, 2 H), 5.29 (AB, *J* = 12 Hz, 4 H), 6.01 (d, *J* = 12 Hz, 2 H), 6.36 (t, *J* = 2 Hz, 2 H), 6.49 (d, *J* = 2 Hz, 4 H), 7.08 (d, *J* = 8 Hz, 1 H), 7.63 (broad s, 1 H), 7.81 (AB, *J* = 8 Hz, 2 H), 7.97 (dd, *J* = 8 and 2 Hz, 1 H), 8.11 (d, *J* = 8 Hz, 1 H), 8.13 (d, *J* = 2 Hz, 1 H), 8.20 (d, *J* = 8 Hz, 1 H), 8.29 (d, *J* = 8 Hz, 1 H), 8.36 (d, *J* = 8 Hz, 1 H), 8.39 (broad s, 2 H). ¹³C NMR (50 MHz, CDCl₃): 9.9, 14.0, 14.1, 22.7, 25.3, 26.1, 26.3, 29.3, 29.4, 29.5, 29.6, 29.7, 30.1, 31.9, 36.9, 49.1, 66.9, 67.5, 68.1, 68.7, 69.1, 69.6, 70.6, 73.3, 101.6, 107.1, 113.3, 113.6, 119.9, 120.9, 124.2, 125.5, 125.6, 126.5, 127.6, 128.2, 132.4, 134.4, 135.8, 136.1, 136.6, 136.8, 137.0, 137.2, 137.9, 140.0, 141.0, 141.1, 142.3, 142.7, 143.2, 143.6, 143.7, 143.9, 144.2, 144.3, 144.6, 144.9, 145.2, 145.3, 145.6, 145.7, 146.1, 147.4, 148.7, 149.3, 150.9, 155.2, 156.9, 160.4, 162.6, 162.7. FAB-MS: 2568.1 (MH⁺, calcd for C₁₇₈H₁₇₇O₁₄N₂: 2568.3). Anal. Calcd for C₁₇₈H₁₇₆O₁₄N₂: C 83.27, H 6.91, N 1.09. Found: C 83.10, H 6.90, N 1.08.

Compound Cu. A solution of Cu(CH₃CN)₄.BF₄ (16 mg, 0.05 mmol) in CH₃CN (5 mL) was added under an argon atmosphere at room temperature to a stirred, degassed solution of **5** (90 mg, 0.08 mmol) in CH₂Cl₂ (10 mL). The solution turned dark red instantaneously, indicating the formation of the complex. After 1 h, the solvents were evaporated. Column chromatography on SiO₂ (CH₂Cl₂/

5% MeOH) yielded **Cu** (92 mg, 96%) as a dark red glassy compound. ^1H NMR (200 MHz, CDCl_3): 0.85–1.60 (m, 168 H), 1.76 (m, 8 H), 3.20 (t, $J = 6$ Hz, 4 H), 3.64 (t, $J = 6$ Hz, 4 H), 3.95 (s, 8 H), 6.04 (d, $J = 8$ Hz, 2 H), 6.95 (m, 6 H), 7.38 (m, 4 H), 7.82 (d, $J = 8$ Hz, 2 H), 7.86 (d, $J = 8$ Hz, 2 H), 7.96 (AB, $J = 8$ Hz, 4 H), 8.44 (d, $J = 8$ Hz, 4 H), 8.46 (d, $J = 8$ Hz, 4 H). ^{13}C NMR (50 MHz, CDCl_3): 11.8, 14.1, 22.7, 25.7, 26.1, 29.1, 29.4, 29.5, 29.6, 29.7, 31.9, 64.2, 68.8, 69.1, 111.6, 113.5, 121.3, 123.9, 124.4, 124.5, 124.9, 126.0, 126.6, 127.7, 128.0, 131.1, 137.0, 138.1, 141.2, 143.3, 143.5, 147.8, 150.1, 156.4, 156.8. Anal. Calcd for $\text{C}_{136}\text{H}_{216}\text{O}_8\text{Si}_4\text{N}_4\text{CuBF}_4$: C 71.09, H 9.47, N 2.44. Found: C 70.96, H 9.51, N 2.31.

Compound F–Cu–F. A solution of $\text{Cu}(\text{CH}_3\text{CN})_4\cdot\text{BF}_4$ (6 mg, 0.02 mmol) in CH_3CN (2 mL) was added under an argon atmosphere at room temperature to a stirred, degassed solution of **12** (80 mg, 0.03 mmol) in CH_2Cl_2 (10 mL). After 1 h, the solvents were evaporated. Column chromatography on SiO_2 (CH_2Cl_2) yielded **F–Cu–F** (76 mg, 92%) as a dark red glassy compound. ^1H NMR (400 MHz, CDCl_3): 0.71–1.70 (m, 276 H), 3.19 (m, 2 H), 3.40 (m, 2 H), 3.64–3.90 (m, 20 H), 4.43 (d, $J = 12$ Hz, 2 H), 4.57 (d, $J = 12$ Hz, 2 H), 4.99 (d, $J = 12$ Hz, 2 H), 5.21 (d, $J = 12$ Hz, 2 H), 5.30 (d, $J = 12$ Hz, 2 H), 5.46 (d, $J = 12$ Hz, 2 H), 5.58 (d, $J = 12$ Hz, 4 H), 6.28 (t, $J = 2$ Hz, 4 H), 6.37 (d, $J = 8$ Hz, 2 H), 6.44 (d, $J = 2$ Hz, 4 H), 6.47 (d, $J = 2$ Hz, 4 H), 6.50 (m, 2 H), 7.20 (broad s, 2 H), 7.30 (broad s, 2 H), 7.34 (dd, $J = 8$ and 2 Hz, 2 H), 7.38 (d, $J = 2$ Hz, 2 H), 7.85 (d, $J = 8$ Hz, 2 H), 8.17 (d, $J = 8$ Hz, 2 H), 8.19 (AB, $J = 8$ Hz, 4 H), 8.55 (d, $J = 8$ Hz, 2 H), 8.56 (d, $J = 8$ Hz, 2 H). ^{13}C NMR (50 MHz, CDCl_3): 14.1, 22.7, 26.1, 29.3, 29.4, 26.4, 29.7, 31.9, 50.1, 65.6, 67.0, 68.1, 68.7, 68.9, 69.3, 70.7, 101.9, 107.0, 107.2, 112.6, 127.8, 128.2, 131.4, 135.5, 135.8, 136.2, 136.4, 136.5, 137.8, 139.6, 141.1, 141.2, 142.2, 142.7, 142.8, 143.3, 143.6, 143.8, 143.9, 144.2, 144.3, 144.7, 144.9, 145.3, 145.5, 145.7, 145.8, 146.0, 146.2, 147.5, 148.5, 148.9, 149.3, 150.4, 156.1, 156.5, 160.3, 160.4, 162.5, 162.6, 162.7. MALDI-TOF-MS: 5198.6 ($[\text{M} - \text{BF}_4^-]^+$, calcd for $\text{C}_{356}\text{H}_{352}\text{O}_{28}\text{N}_4\text{Cu}$: 5198.3). Anal. Calcd for $\text{C}_{356}\text{H}_{352}\text{O}_{28}\text{N}_4\text{CuBF}_4$: C 80.91, H 6.71, N 1.06. Found: C 80.81, H 6.93, N 1.02.

Molecular Modeling. The Molecular Dynamics studies have been performed on SGI Origin 200 and Octane² workstations using the Discover 3 software from Accelrys (www.accelrys.com) with the pcff force field. The previously minimized structures were allowed to equilibrate for 500 ps at a 300 K isotherm by the MD simulation (in the NVT ensemble with a time step of 1 fs).

Electrochemistry. The electrochemical studies were carried out in CH_2Cl_2 (Fluka, spectroscopic grade used without further purification) containing 0.1 M Bu_4NPF_6 (Merck, electrochemical grade) as supporting electrolyte. A classical three electrode cell was connected to a computerized electrochemical device Autolab (Eco Chemie B. V. Utrecht, Holland) driven by GPSE software running on a personal computer. The working electrode was a glassy carbon disk (3 mm in diameter), the auxiliary electrode a platinum wire and the reference electrode an aqueous Ag/AgCl reference electrode. All potentials are given versus Fc/Fc^+ used as internal standard.

Photophysical Measurements. The spectroscopic investigations were carried out in CH_2Cl_2 (Carlo Erba, spectrofluorimetric grade).

The samples were placed in fluorimetric 1 cm path cuvettes and, when necessary, purged from oxygen by four freeze–pump–thaw cycles at 2×10^{-6} Torr. Absorption spectra were recorded with a Perkin-Elmer $\lambda 40$ spectrophotometer. Uncorrected emission spectra were obtained with a Spex Fluorolog II spectrofluorimeter (continuous 150 W Xe lamp), equipped with a Hamamatsu R-928 photomultiplier tube. The corrected spectra were obtained via a calibration curve determined with a procedure described earlier.³³ Fluorescence quantum yields obtained from spectra on an energy scale (cm^{-1}) were measured with the method described by Demas and Crosby⁵⁴ using as standards an air-equilibrated solution of $[\text{Os}(\text{phen})_3]^{2+}$ in acetonitrile ($\Phi_{\text{em}} = 0.005$).⁵⁵

The steady-state IR luminescence spectra were obtained with an Edinburgh FLS920 spectrometer equipped with Hamamatsu R5509-72 supercooled photomultiplier tube (193 K) and a TM300 emission monochromator with NIR grating blazed at 1000 nm. An Edinburgh Xe900 450 W xenon arc amp was used as light source. The determination of the relative yields of singlet oxygen sensitization for **F** and **Cu–F** was obtained by monitoring the intensity of the steady-state singlet oxygen luminescence at 1270 nm.⁵⁶ Solutions with the same optical density and solvent (CH_2Cl_2) were used, making corrections due to these factors unnecessary.⁵⁶

Emission lifetimes in the nanosecond and picosecond time scale were determined with an Edinburgh FLS920 time correlated single photon counting spectrometer. The light source is a Hamamatsu PLP-02 SLDH-041 laser diode working at 1 MHz repetition rate ($\lambda_{\text{exc}} = 405$ nm, 40 ps pulse width); the detector was a red-sensitive Peltier cooled Hamamatsu R-928 photomultiplier tube. The time resolution of the system is 30 ps after deconvolution.

The fullerene triplet lifetimes were obtained by using the second harmonic (532 nm) of a Nd:YAG laser (JK Lasers) with 20 ns pulse and 1–2 mJ of energy per pulse. The details on the flash-photolysis system are reported elsewhere.⁵⁷

Experimental uncertainties are estimated to be $\pm 8\%$ for lifetime determinations, $\pm 20\%$ for emission quantum yields, $\pm 5\%$ for relative emission intensities in the NIR, and ± 1 nm and ± 5 nm for absorption and emission peaks, respectively.

Acknowledgment. This research was supported by the CNR, the CNRS, the French Ministry of Research (ACI Jeunes Chercheurs), and the EU for the RTN Contract HPRN-CT-2002-00171. Y.R. thanks the Direction de la Recherche of the French Ministry of Research and G.A. the Spinner Agency (Regione Emilia-Romagna, Italy) for their fellowships. We further thank L. Oswald for technical help, M. Schmitt for high field NMR spectra, and J.-M. Strub for MS measurements.

IC0351460

(54) Demas, J. N.; Crosby, G. A. *J. Phys. Chem.* **1971**, *75*, 991.

(55) Kober, E. M.; Caspar, J. V.; Lumpkin, R. S.; Meyer, T. J. *J. Phys. Chem.* **1986**, *90*, 3722.

(56) Wirp, C.; Gusten, H.; Brauer, H. D. *Ber. Bunsen-Ges. Phys. Chem.* **1996**, *100*, 1217.

(57) Flamigni, L. *J. Phys. Chem.* **1992**, *96*, 3331.